SEASONAL AND INTERANNUAL VARIABILITY OF SURFACE HEAT AND FRESHWATER FLUXES IN THE MEDITERRANEAN SEA: BUDGETS AND EXCHANGE THROUGH THE STRAIT OF GIBRALTAR

Francisco Criado-Aldeanueva[(1)], F. Javier Soto-Navarro[(1)], Jesús García-Lafuente[(1)]

(1) Physical Oceanography Group, Department of Applied Physics II, University of Málaga, Málaga, Spain.

Corresponding author:

Francisco Criado Aldeanueva

Dpto. Física Aplicada II, Universidad de Málaga

29071 Málaga, Spain

Tel.: +34 952 132849, Fax: +34 952 131355

fcaldeanueva@ctima.uma.es

SEASONAL AND INTERANNUAL VARIABILITY OF SURFACE HEAT AND FRESHWATER FLUXES IN THE MEDITERRANEAN SEA: BUDGETS AND EXCHANGE THROUGH THE STRAIT OF GIBRALTAR

ABSTRACT: Several NCEP climatological datasets have been combined to analyse the seasonal and interannual variations of the heat and water budgets in the Mediterranean Sea and compare the long term means with direct measurements in the Strait of Gibraltar. The seasonal cycle of the net heat is positive (toward the ocean) between March and September with maximum in June and negative the rest of the year with minimum in December. Although subject to inherent uncertainty, we obtain a practically neutral budget of 0.7 Wm^{-2} in a yearly basis. The net heat budget is positive for the western Mediterranean (~12 Wm^{-2}) and negative for the eastern Mediterranean (~ -6.4 Wm^{-2}) mainly due to the high latent heat losses of this basin. The E-P freshwater deficit has a seasonal cycle with a range of variation about 600 $mm\cdot y^{-1}$, maximum in August-September and minimum in May. The long-term mean of the basin-averaged deficit is 680±70 $mm\cdot y^{-1}$ but it is almost 70% greater in the eastern Mediterranean due to higher E and lower P in this basin. Combining the climatological values with in situ measurements in Espartel sill, a mean inflow through the Strait of Gibraltar of 0.82±0.05 Sv is obtained and a salinity ratio S_{in}/S_{out} = 0.956. A heat advection Q_a = 3.2±1.5 Wm^{-2} through the Strait of Gibraltar has been obtained that, combined with the long-term averaged surface heat flux, implies that the net heat content of the Mediterranean Sea would have increased in the last decades.

Keywords: Mediterranean Sea, heat and freshwater fluxes, seasonal and interannual variability, Strait of Gibraltar.

1.- INTRODUCTION

The Mediterranean Sea (Figure 1), a semi-enclosed basin that extends over 3000 km in longitude and over 1500 km in latitude with an area of $2.5 \cdot 10^{12}$ m^2, communicates with the Atlantic Ocean through the Strait of Gibraltar and with the Black Sea through the Turkish Bosphorus and Dardanelles Straits. The Sicily Channel separates the western and eastern Mediterranean basins. Evaporative losses (E) are not balanced by precipitation (P) and river runoff (R) and an Atlantic inflow through the Strait of Gibraltar is necessary to balance the freshwater and salt budgets. The Atlantic Water (AW) becomes saltier and denser while spreading into the western and eastern basins under the influence of intense air-sea interactions. Most of this flow returns to the Atlantic Ocean as Levantine Intermediate Water (LIW), formed during winter convection in the Levantine subbasin, while another part is transformed into Eastern Mediterranean Deep Water (EMDW) in the Adriatic and the Aegean subbasins and into Western Mediterranean Deep Water (WMDW) in the Gulf of Lions, the latter eventually being part of the Gibraltar outflow (Bryden and Stommel, 1982; Astraldi et al., 2002; Millot et al., 2006; García-Lafuente et al., 2007, 2009). All processes of deep water formation involve LIW in less or greater extent, which makes all water masses be closely related and any significant modification of one of them may propagate its effect to the others. For this reason, the freshwater flux through the Mediterranean Sea surface plays an important role in the exchange between the Atlantic and the Mediterranean.

-----------------------------Approximate location of Figure 1-----------------------------------

A great number of studies have dealt with the Mediterranean water budget (Bethoux, 1979; Peixoto et al., 1982; Bryden and Kinder, 1991b; Harzallah et al., 1993; Gilman and Garrett, 1994; Castellari et al., 1998; Angelucci et al., 1998; Béthoux and Gentili, 1999; Boukthir and Barnier, 2000; Mariotti et al., 2002) but, despite these efforts, the estimate of the freshwater flux at the surface has showed to depend on the datasets used and the methodology applied and remains largely uncertain, in particular its seasonal and interannual variability. For instance, estimates of E-P are found to range from 421 $mm \cdot y^{-1}$ (Gilman and Garrett, 1994) to 1230 $mm \cdot y^{-1}$ (Béthoux and Gentili, 1999), confirming the difficulty of obtaining a reliable estimate.

Air-sea heat fluxes are closely related to the water budget. The net heat budget consists of two radiation components (solar shortwave radiation absorbed by the sea and longwave radiation emitted by the sea) and two turbulent contributions (latent and sensible heat fluxes). In the long-term, vertical heat fluxes integrated over the basin must be balanced by heat transport through the Strait of Gibraltar. Macdonald et al. (1994), using in situ current and temperature observations estimated an annual average heat transport from the Atlantic to the Mediterranean of 5.2±1.3 Wm^{-2}. Other authors have also obtained the long-term heat flux through Gibraltar from estimates of the volume transport and the temperatures of the inflow and outflow. Results range from 8.5 Wm^{-2} (Béthoux, 1979) to 5 Wm^{-2} (Bunker et al., 1982). Since the uncertainty of these results is rather low, they can be used as a reference for the evaluation of the surface heat flux budget. Several studies (Bunker et al., 1982; Garrett et al., 1993; Schiano et al., 1993; Gilman and Garrett, 1994) have compared long term averages of vertical heat fluxes with the heat transport through the Strait of Gibraltar obtaining discrepancies of up to 30 Wm^{-2}. The reasons given for the disagreement are the different periods covered and the different bulk formula parameterisations or the wind forcing fields (Ruti et al., 2008). More recently, Ruiz et al. (2008) have examined 44 years (1958-2001) of HIPOCAS model data to report a value of 1 Wm^{-2} for the vertical heat flux (heat loss from the ocean). They attribute the difference with respect to the heat gain through the Strait to an increase in the net heat content of the Mediterranean Sea during the last decades.

Semi-enclosed basins such as the Mediterranean are suitable for the characterisation of heat and water fluxes since they make a budget closure feasible. In this work we combine several datasets to analyse the seasonal and interannual variations of the components of heat and water budgets and compare the long term means with direct measurements in the Strait of Gibraltar. This double climatological and *in situ* approach makes it possible to provide an indirect determination of the inflow through the Strait of Gibraltar in a reliable way. The work is organised as follows: section 2 describes the data and methodology; in section 3 the main results are presented and discussed both for the heat and water fluxes. Budgets and the exchange through the Strait of Gibraltar are also addressed. Finally, section 4 summarises the conclusions.

2.- DATA

Monthly means from January 1948 to February 2009 of precipitation, evaporation and surface heat fluxes have been retrieved from the National Center for Enviromental Prediction-National Center of Atmospheric Research (NCEP-NCAR) reanalysis project (NCEP hereinafter, Kalnay et al., 1996), which is run at T62 spectral resolution (approximately a grid size of 1.9ºx1.9º) with 28 sigma levels. For comparison purposes, data from the Climate Prediction Centre Merged Analysis of Precipitation (CMAP, Xie and Arkin, 1996, 1997) have also been analysed. This dataset gives estimation of monthly mean precipitation at 2.5ºx2.5º resolution for the period 1979-2009. The standard version consists in a merged analysis mainly based on gauge stations over land and satellite estimates over the ocean. Auxiliary data of monthly mean sea level pressure, air temperature and wind fields at 2.5ºx2.5º for the period 1948-2009 have also been retrieved from NCEP database. Seasonal means have been computed by averaging JFM (winter), AMJ (spring), JAS (summer) and OND (autumn) monthly data.

Sea Surface Temperature (SST) data have been obtained from the Advanced Very High Resolution Radiometer (AVHRR) Pathfinder v5 mission of the NASA Jet Propulsion Laboratory (JPL). They consist in infrared high resolution radiometer images with 4km x 4km spatial resolution acquired onboard several satellite missions. Monthly means between 1985 and 2007 have been analysed.

In situ measurements of the outflow through the Strait of Gibraltar have been collected in the frame of the INGRES 1-2 projects. Data from a CT probe placed over Espartel sill, at 35º 51.70N, 5º 58.60W and 5 m above the seafloor between September 2004 and December 2009 have been used in this work to characterise its temperature. MEDATLAS database provided historical Conductivity-Temperature-Depth (CTD) profiles over Espartel in order to determine the inflow properties. The region within 35º 48.6'N – 35º 53.9'N / 05º 56.7'W – 06º 00.8'W (see Figure 1B) has been considered to be representative for the Espartel area. 48 CTD profiles spanning all seasons have been identified, most of them from the field work carried out during the Gibraltar Experiment (1986).

3.- RESULTS AND DISCUSSION

3.1.- Air and sea surface temperature fields

The spatial distribution of climatological sea level air temperature over the Mediterranean basin for 1948-2009 (Figure 2A) exhibits a north-south gradient with lower temperatures (below 10ºC) in the European coasts that progressively increase up to 22ºC in the African coasts. The eastern basin is warmer than the western one in all seasons, with maxima above 25ºC in the Levantine subbasin in summer. Minimum values between 5ºC-7ºC are found in the Adriatic, Aegean and Gulf of Lions in winter (not shown). The yearly time series of the basin-averaged air temperature (Figure 2B) has a mean value of 16.9ºC with minimum in 1956 (16.2ºC) and maximum in 1994 (17.7ºC). A positive trend of 0.012±0.003 $ºC \cdot y^{-1}$ is obtained but it nearly doubles if only the period from 1956 onwards is considered. Positive anomalies concentrate in the last decades and negative ones during the 60s and 70s. The Ionian subbasin is particularly sensitive to this positive trend with values above 0.02 $ºC \cdot y^{-1}$ for the whole period (Figure 2C).

-----------------------------Approximate location of Figure 2-----------------------------------

A similar pattern is observed for the climatological SST spatial distribution for 1985-2007 (Figure 2D) with temperatures increasing from north to south and from west to east. The Levantine subbasin and the south Ionian are warmer areas, with temperatures up to 28ºC in summer. In the western basin, warmer areas are located in the Algeric-Balearic region and the south-east Tyrrhenian. The Aegean, the northern Adriatic and the Gulf of Lions are again the coldest subbasins, with temperatures averaging 10ºC in winter. The yearly time series of the Mediterranean-averaged SST (Figure 2E) has a mean value of 17.8ºC and a positive trend of 0.05 ± 0.01 $ºC\cdot y^{-1}$ for the period 1985-2007, slightly lower than the one obtained by Criado-Aldeanueva et al. (2008) for 1992-2005 and significantly lower than the 0.15 $ºC\cdot y^{-1}$ obtained by Marullo et al. (1999) for the period 1982-1990. The discrepancy may be due to the possibility mentioned by Moron (2003) that the trend had changed sign after reaching a SST relative maximum in year 2000, although the very hot years 2003 and 2008 shed doubts on the conclusion of Moron (2003). Mariotti et al (2008) and Mariotti (2010) analyze SST trends for various sub-periods between 1960 and 2005 and report decadal variations that follow those of the air temperature even though longer series are necessary to establish conclusions. SST trend (Figure 2F) is positive elsewhere with higher values in the eastern basin, especially south of Crete (up to 0.08±0.02 $ºC\cdot y^{-1}$ for the period analysed). Fenoglio-Marc (2002) and Cazenave et al. (2002) report negative trends in the western Ionian for the periods 1992-2000 and 1993-1998 respectively, which change sign when considering longer time series as in Criado-Aldeanueva et al. (2008). Superposed to these linear trends, both air temperature and SST show a very marked seasonal cycle (not shown), the former leading the latter by 15-20 days (maximum in mid-July).

3.2.- Surface heat fluxes in the Mediterranean Sea

3.2.1.- Spatial climatologies and seasonal cycle

Figure 3 displays the seasonal climatology of the different components of the net heat budget. Sensible heat flux, Q_h (panel A) concentrate higher losses during autumn and winter with maxima above 60 Wm^{-2} in the Aegean and Adriatic and slightly lower values in the Gulf of Lions and the Levantine subbasin (~50 Wm^{-2}). Elsewhere, the spatial distribution is rather uniform in these seasons with losses of some 20 Wm^{-2}. Heat gains up to 20 Wm^{-2} occur in spring and summer in the Aegean, the Levantine subbasin and some areas of the north-African coasts. Latent heat flux, Q_e (panel B) is larger in the eastern basin with losses up to 160 Wm^{-2} in the Levantine area in autumn and winter. In the western Mediterranean, the highest losses are located in the Gulf of Lions and the Balearic subbasin (~130 Wm^{-2}). Minimum fluxes take place in spring with a more uniform spatial distribution and lower values in the Adriatic and the westernmost area (~20 Wm^{-2}). The solar shortwave net radiation, Q_s (panel C) depicts a north-south, west-east gradient in all seasons, with maxima in spring in the Levantine subbasin (more than 250 Wm^{-2}) and minima in autumn in the western European coasts (~50 Wm^{-2}). The longwave net radiation Q_b (panel D) is rather independent of seasonal variations. Higher losses of some 90 Wm^{-2} concentrate in summer in the Aegean Sea and Levantine subbasin whereas lower values correspond to the Balearic and Tyrrhenian subbasins in spring (~60 Wm^{-2}). The combination of these four contributions produces a marked seasonal-dependent net heat flux Q_n (not shown), with losses in autumn and winter and gains in spring and summer. Higher losses are observed in the Levantine subbasin, the Aegean, the northern Adriatic and the Gulf of Lions (>150 Wm^{-2}) in autumn, that favours the formation of intermediate and deep waters in these areas (Tziperman and Speer 1994; Candela 2001; Schroeder 2009). Mean values for each contribution in the eastern and western basins are presented for all seasons in Table 1.

-----------------------------Approximate location of Figure 3----------------------------------

-----------------------------Approximate location of Table 1-----------------------------------

The Mediterranean-averaged climatological seasonal cycle for each component is presented in Figure 4. For the sensible heat flux Q_h, the values are negative all year round, with a range of variation of 34 Wm^{-2}, a maximum of -2 Wm^{-2} in June and a minimum of -36 Wm^{-2} in December. The latent heat flux Q_e, is minimum (-125 Wm^{-2}) in November and maximum (-50 Wm^{-2}) in May. The seasonal cycle of the shortwave radiation Q_s, positive all the year, has a range of variation of 196 Wm^{-2}, a maximum of 281 Wm^{-2} in June and a minimum of 85 Wm^{-2} in December. Finally, the net longwave radiation Q_b does not exhibit a clear seasonal cycle but a rather uniform value between -75 and -80 Wm^{-2}. These results are in reasonable good agreement with those obtained by Matsoukas et al (2005), who derive the radiative components by a radiation transfer model instead of bulk formulae. The seasonal cycle of the net heat shows positive values (heat gain by the ocean) between March and September with maximum in June (143 Wm^{-2}) and negative values during the rest of the year. It shows a minimum in December (-152 Wm^{-2}) and a range of variation of 295 Wm^{-2}, which is slightly less than the 330 Wm^{-2} obtained by Ruiz et al. (2008) and close to the lower limit of the interval reported by Garrett et al. (1993), 280 Wm^{-2}-360 Wm^{-2}. The obtained phase is in agreement with both works and slightly different from that obtained by Matsoukas et al (2005), who situate the maximum in May. Solar radiation and latent heat are the major contributions to the net heat flux.

-----------------------------Approximate location of Figure 4-----------------------------------

The heat flux Q_n is the time derivative of the heat content H, $Q_n = dH/dt$, responsible of the thermosteric anomaly. If we assume a harmonic function for the annual cycle of Q_n, then H will also have a harmonic shape but delayed $\pi/2$ (3 months) and therefore the thermosteric sea level cycle is expected to peak in September, in agreement with previous works (Fenoglio-Marc et al., 2006; García et al., 2006; Criado-Aldeanueva et al., 2008).

3.2.2.- Basin-averaged annual means and long-term fluctuations

Figure 5A displays the yearly, Mediterranean-averaged, time series of the different contributions and the net heat flux. Solar shortwave radiation is the only positive contribution with a mean value of ~186±4 Wm^{-2}. The other contributions are negative with mean values about -93±6 Wm^{-2}, -77±2 Wm^{-2} and -15±3 Wm^{-2} for latent, longwave and sensible heat, respectively. As a result, we obtain a nearly neutral budget of 0.7 Wm^{-2}. The mean values have also been computed for each basin (Table 1): the net heat budget is positive (~12 Wm^{-2}) for the western Mediterranean and negative for the eastern Mediterranean (~ -6.4 Wm^{-2}) due to the high latent heat losses (up to 100 Wm^{-2}).

The long-term averages of each component are compared with previous estimates in Table 2. The value for shortwave radiation is the same as the one obtained by Matsoukas et al (2005) from a radiation transfer model, a value lower than most previous estimations except for those of Gilman and Garrett (1994) and Ruiz et al. (2008) who computed a contribution 10% lower from 1958-2001 HIPOCAS reanalysis data, probably due to a different parameterisation scheme. The latent heat flux is also lower than previous estimations and similar to that of Matsoukas et al. (2005) and Ruiz et al. (2008), which is thought to be rather accurate due to the higher spatial resolution of HIPOCAS dataset. The value for longwave radiation is the same as the one obtained by Gilman and Garrett (1994) and Castellari et al. (1998) and is close to that of Ruiz et al. (2008). The computed sensible heat flux is greater than all previous estimations, although it is not far from values reported by Bethoux (1979), Bunker et al. (1982) and

Castellari et al. (1998). The net heat flux is in the range of previous studies, especially close to those of May (1986), Gilman and Garrett (1994) and Ruiz et al. (2008).

-----------------------------Approximate location of Figure 5-----------------------------------

-----------------------------Approximate location of Table 2-----------------------------------

Although there is no significant trend in the series, Figure 5B reveals three different periods in the heat flux anomalies: from early 50s to mid 60s, a negative trend of -1.6±0.6 $Wm^{-2}y^{-1}$ is observed. Trend changes to positive (1.1±0.3 $Wm^{-2}y^{-1}$) until late 80s when it changes sign again (-0.9±0.6 $Wm^{-2}y^{-1}$). Maximum heat gain of about 20 Wm^{-2} is observed in 1989 and maximum losses of the same order in 1963 and 2005. Since fluctuations in the net budget do not appear to be random, discrepancies with previous estimations could be related to the different periods analysed. It is interesting to remark that fluctuations in the net heat flux closely follow those of the latent heat (trends of -1.1±0.5 $Wm^{-2}y^{-1}$, 0.7±0.2 $Wm^{-2}y^{-1}$ and -0.7±0.4 $Wm^{-2}y^{-1}$ are observed for the same periods referred above), suggesting that this contribution is the main source of interannual variability. The visual inspection of Figure 5B also suggests a 40-year period multi-decadal oscillation of 11±2 Wm^{-2} and 7.5±1.4 Wm^{-2} amplitude for net and latent heat fluxes, respectively, probably related to long-term atmospheric forcing. However, long-term variability is the less reliable aspect of reanalyses datasets so some caution is necessary here. Although general good agreement is found with the results of Mariotti (2010) based on different datasets, this author reports an increase in the recent period compared to the 1960s (i.e. a trend superposed to the decadal variability) that sheds doubts on the 40-year oscillation. Longer time series will be of great help to clarify this issue.

3.3. - Surface freshwater fluxes in the Mediterranean Sea

3.3.1. - Spatial climatologies and seasonal cycle

Figure 6 displays the spatial distributions of the climatological seasonal mean precipitation (P), evaporation (E) and deficit (E-P). For precipitation (panel A), NCEP data (with higher resolution than CMAP data) are presented. Autumn is the wettest season with a mean value of 853 mm·y^{-1}. Higher precipitations are located in the northern Ionian, the Algerian-Balearic subbasin and the easternmost Levantine subbasin. Summer is the driest season (245 mm·y^{-1}), with drier areas along the African coasts. In spring and summer, higher precipitations concentrate in the northern Adriatic. CMAP data (not shown) provide similar results (slightly lower values in all seasons). These patterns are in good agreement with the description of Mariotti et al. (2002) but values are significantly higher than those of Boukthir and Barnier (2000) from ECMWF ERA-15 (1979-1993) dataset.

Based on List (1951), evaporation (panel B) has been computed from the latent heat losses, Q_e and SST according to:

$$E = \frac{Q_E}{\rho L} \qquad [1]$$

where ρ is the sea water density and $L = [2.501 - 0.00237 \cdot SST(^{\circ}C)] \cdot 10^{6}$ J·kg^{-1} the latent heat of vaporization. As the relative importance of the SST term is negligible, evaporation matches the spatial patterns of latent heat flux. It is more intense in autumn due to the strong and dry winds, with a mean value of 1553 mm·y^{-1}, maximum about 2000 mm·y^{-1} in the southern Ionian and Levantine subbasins and lower values in spring

(745 mm·y^{-1}). In all seasons, evaporation is ~30% higher in the eastern basin except in autumn (only 13% higher). In the western Mediterranean, the Balearic subbasin shows the highest values. These patterns are in good agreement with those of Mariotti et al. (2002) but evaporation is higher than the values reported by Boukthir and Barnier (2000). Mariotti et al. (2002) compare both NCEP and ERA-15 datasets and conclude that the latter tends to underestimate both P and E with respect to NCEP.

E-P (panel C) is positive (freshwater deficit) for most of the Mediterranean during all seasons, especially in the eastern basin due to higher evaporation and lower precipitation. Some areas of the western basin change sign seasonally and, in the northern Adriatic, E-P is predominantly negative (freshwater input) due to the high precipitation (see panel A). Mean values are positive for all seasons and a maximum of 974 mm·y^{-1} is reached in summer in NCEP data (in autumn in NCEP (E)/CMAP (P) data, 922 mm·y^{-1}). The minimum is observed in spring in both datasets (495 mm·y^{-1} and 418 mm·y^{-1} for NCEP and NCEP/CMAP, respectively). Higher deficits concentrate in the Levantine subbasin in summer (1800 mm·y^{-1}) and higher inputs in the northern Adriatic during spring (-400 mm·y^{-1}). In all season, E-P is lower in NCEP data due to higher precipitation of this dataset with respect to CMAP. Table 3 summarises the above results.

-----------------------------Approximate location of Figure 6-----------------------------------

-----------------------------Approximate location of Table 3-----------------------------------

The Mediterranean-averaged climatological seasonal cycles of E, P and E-P (NCEP and CMAP) are presented in Figure 7. A range of variation of 838 mm·y^{-1} is obtained in the NCEP precipitation data, with a maximum (959 mm·y^{-1}) in December and a minimum (121 mm·y^{-1}) in July. CMAP data are slightly lower in the second half of the year and

~100 mm·y^{-1} higher in spring. Its minimum coincides with that of NCEP and its maximum is somewhat lower (854 mm·y^{-1} in December). The spatial distribution of annual amplitude, (max-min)/2, is rather variable (Figure 8A, NCEP data) with maxima between 650 mm·y^{-1} and 850 mm·y^{-1} in the northern Ionian, the Levantine subbasin and some points of the Algerian subbasin. The phase distribution (not shown) peaks in December in most of the Mediterranean except some reduced areas (mostly in the Levantine subbasin) where it does peak in January. CMAP data (Figure 8B) gives lower values almost everywhere except in the northern Levantine subbasin.

The evaporation seasonal cycle (Figure 7) leads ~2 months that of precipitation and reaches its minimum in May (650 mm·y^{-1}) and its maximum in November (1614 mm·y^{-1}). The amplitude, (max-min)/2, is between 500 mm·y^{-1} and 650 mm·y^{-1} with lower values in the northern areas of the western basin (Figure 8C). The phase distribution (not shown) is also rather uniform with a maximum in November except for some isolated points where it moves to October or to December.

The E-P seasonal cycle (Figure 7) has a range of variation between 582 mm·y^{-1} (NCEP) and 644 mm·y^{-1} (NCEP/CMAP) with a maximum in August-September (~1000 mm·y^{-1}) and a minimum in May, ~100 mm·y^{-1} lower in NCEP/CMAP data. The highest amplitudes, (max-min)/2, concentrate in the Levantine subbasin and lower values are observed in the central Mediterranean (Figure 8D) with a good agreement between NCEP and NCEP/CMAP distributions although the latter gives higher values (Figure 8E). Good agreement is also found in the phase pattern (only NCEP is shown, Figure 8F) that peaks between July and November with a rather irregular spatial distribution.

The seasonal cycles are in reasonably good agreement with the results of Mariotti et al. (2002). Lower amplitudes are reported by Boukthir and Barnier (2000) from ERA-15 and maximum evaporation is obtained in September instead of November. Mariotti (2010) has analysed how long-term changes in E and P affect the mean seasonal cycles. For E-P noticeable changes are observed when comparing with the 1996-2005 period. For these years, the seasonal cycle clearly peaks in September and reaches a relative maximum in February that is not observed for previous time periods. The author attributes these changes to E increase for the September peak and to P decrease for the February peak.

-----------------------------Approximate location of Figure 7-----------------------------------

-----------------------------Approximate location of Figure 8---------------------------------

3.3.2. – Basin-averaged annual means and long-term oscillations

Figure 9A displays the Mediterranean-averaged time series of E, P and E-P. From NCEP data, the long-term mean precipitation is 506 ± 66 $mm \cdot y^{-1}$ with a maximum in 1966 (617 $mm \cdot y^{-1}$), a minimum in 1989 (355 $mm \cdot y^{-1}$) and a negative trend of -1.1 ±0.9 $mm \cdot y^{-2}$, similar to that reported by Mariotti (2010). At the decadal scale, however, three 20-year periods of different trend are revealed: 1948-69 (4±2 $mm \cdot y^{-2}$), 1969-89 (-8±4 $mm \cdot y^{-2}$) and 1989-2008 (9±4 $mm \cdot y^{-2}$). From CMAP data, a slightly lower average value is obtained (469 ± 66 $mm \cdot y^{-1}$). Although both datasets provide fairly similar series until late 90s, they considerably differ (about 100 $mm \cdot y^{-1}$) from 2002 to 2008. The 60-year mean evaporation is 1186 ± 81 $mm \cdot y^{-1}$ with a maximum of 1360 $mm \cdot y^{-1}$ in 2003 and a minimum of 1000 $mm \cdot y^{-1}$ in 1989. The time-evolution of positive and negative anomalies follow that of P and the same three 20-year periods apply for E as well with trends of 8±4 $mm \cdot y^{-2}$, -7±3 $mm \cdot y^{-2}$ and 9±5 $mm \cdot y^{-2}$, respectively that suggests the existence of a multi-decadal oscillation that could be related to long-term atmospheric forcing (Figure 9B). A least-squares fit provides amplitudes of 69±21 mm·y^{-1} and 95±18 mm·y^{-1} at 40 years period for P and E, respectively.

The long-term E-P mean deficit is 680 ± 70 (678 ± 75 from NCEP/CMAP) with a maximum of 817 mm·y^{-1} in 2001 and a minimum of 530 mm·y^{-1} in 1951. A positive trend (higher deficit) of 1.6±0.9 mm·y^{-2} is observed for the entire period in which the decrease in P accounts for ~70%. The multi-decadal E-P oscillation is not so clear (Figure 9B, bottom) and is more likely to correspond to multi-decadal variability and a positive trend as pointed by Mariotti (2010). The decadal variations in E reported here are consistent with those found by Mariotti (2010), although this author finds an increase in E in the recent period compared to the 1960s (i.e. a trend superposed to the decadal variability). In contrast, precipitation decrease based on NCEP found here is too large compared with estimates based on land-gauges around the Mediterranean reported in Mariotti (2010). This is also reflected in our conclusion that 70% of the recent increase in E-P derives from P, while Mariotti (2010) underlines the role of evaporation changes. As previously pointed out, long-term variability is the less reliable aspect of reanalyses datasets, so our results must be considered here with caution.

-----------------------------Approximate location of Figure 9---------------------------------

Mean values have also been computed for each basin and are displayed in Table 3. E-P is almost 70% higher in the eastern Mediterranean due to higher E and lower P in this basin. We now compare these results with previous estimations (Table 4). E ranges from 920 mm·y^{-1} to 1570 mm·y^{-1}. The two lowest estimates (Mariotti et al., 2002 and Boukthir and Barnier, 2000) use the ERA-15 reanalyses whereas the highest of Castellari et al. (1998) and Bethoux and Gentili (1999) derive from observations. Our result is an intermediate value close to those of Mariotti et al. (2002) from NCEP dataset although for different time periods. P ranges 310 mm·y^{-1} to 700 mm·y^{-1}. Again, the values from ERA-15 are among the lowest ones. Our result (from NCEP) is slightly higher than most of the previous perhaps due to the increase of P in the most recent years (see the positive trend in Figure 9B). Our result for E-P falls within the range of previous estimates (from 421 mm·y^{-1} to 1230 mm·y^{-1}) and is especially close to those of Mariotti et al. (2002) from different datasets and periods analysed.

-----------------------------Approximate location of Table 4-----------------------------------

3.4.- Budgets and exchange through the Strait of Gibraltar

Should the Mediterranean be in a steady state, the net water and heat transport through the straits (horizontal advection) must balance the vertical fluxes integrated over the basin. The first condition can be written as:

$$G = \int\int (E - P)dxdy - R - B \qquad [2]$$

where $G = G_{in} - G_{out}$ is the net flow through the Strait of Gibraltar (the difference between inflow G_{in} and outflow G_{out}) , R is the total river runoff and B the contribution of the Black Sea.

Several studies (Tixeront, 1970; Ovchinnikov, 1974; Margat, 1992; Boukthir and Barnier, 2000; Struglia et al., 2004) have dealt with the determination of climatological river discharge into the Mediterranean Sea using different methodologies and have obtained different results. Boukthir and Barnier (2000), analysing data from UNESCO (1996) for the period 1974-94 reported a climatological mean of 11·10^3 m^3·s^{-1}, 30% lower than the estimates of Tixeront (1970) based on rain maps and data from a few coastal stations, Ovchinnikov (1974), who gave 13.6·10^3 m^3·s^{-1} or Margat (1992), who proposed $16 \cdot 10^3$ $m^3 \cdot s^{-1}$ from a global hydrological budget of the Mediterranean basin. Struglia et al. (2004), analysing data from Global Runoff Data Center (GRDC) and the Mediterranean Hydrological Cycle Observing System (Med-HYCOS), reported an annual mean climatological value of $8.1 \cdot 10^3$ $m^3 \cdot s^{-1}$ and mentioned $10.4 \cdot 10^3$ $m^3 \cdot s^{-1}$ as an upper bound to possible underestimates. This last value is close to that of Boukthir and Barnier (2000) and will be adopted for our calculations. In any case, a contribution of river discharge of $10.4 \cdot 10^3$ $m^3 \cdot s^{-1}$ (equivalent to 131 $mm \cdot y^{-1}$) is less than 20% of the more important E-P.

The Black Sea contribution has also been extensively studied (Tolmazin, 1985; Unluata et al., 1990; Besiktepe et al., 1994, Bethoux and Gentili, 1999; Karnaska and Maderich, 2008; Liu et al., 2009). Results range from $5.8 \cdot 10^3$ $m^3 \cdot s^{-1}$ of Bethoux and Gentili (1999) from the hydrological budget in the Aegean, to $9.6 \cdot 10^3$ $m^3 \cdot s^{-1}$ of Liu et al. (2009) from numerical simulation, which is close to those of Unluata et al. (1990) and Besiktepe et al. (1994). Karnaska and Madirich (2008), from a 3D model obtain mean annual values of $38.8 \cdot 10^3$ $m^3 \cdot s^{-1}$ for the upper layer (into the Mediterranean Sea) and $30.0 \cdot 10^3$ $m^3 \cdot s^{-1}$ for the lower layer (into the Black Sea) and hence a mean net inflow of $8.8 \cdot 10^3$ $m^3 \cdot s^{-1}$. This intermediate value will be adopted for our calculations. Thus, the contribution of the Black Sea (equivalent to 111 $mm \cdot y^{-1}$) is similar to the river runoff.

With these values for R and B and the mean value of E-P = 680 $mm \cdot y^{-1}$ discussed above, equation [2] provides a net flow through the Strait of Gibraltar of 0.035 ± 0.005 Sv (Sverdrup, $1Sv = 10^6$ $m^3 \cdot s^{-1}$), in good agreement with previous estimates (see Table 5). Our result is similar to those based on water budgets and slightly lower than that of

Mariotti et al. (2002) from NCEP dataset because we have used more recent values of R and B, which are slightly higher.

-----------------------------Approximate location of Table 5-----------------------------------

Combining a 4 year-long time series of ADCP measurements over Espartel sill with results from a numerical model, Sánchez-Román et al. (2009) report a mean outflow of G_{out} = 0.78 ± 0.05 Sv, which implies a mean inflow ($G_{in} = G + G_{out}$) of 0.82 ± 0.05 Sv. The estimation of the inflow from direct observations has technical and operational limitations and only a few values (that range from 0.72 Sv to 1.2 Sv) have been reported in the literature (see Table 6). Indirect estimations are mainly based on the volume and salt conservation (the well-known Knudsen relationship) and depend on the inflow and outflow salinity (S_{in}, S_{out}, respectively) ratio:

$$G_{in} = \frac{1}{1 - S_{in}/S_{out}} G \qquad G_{out} = \frac{1}{1 - S_{out}/S_{in}} G \qquad [3]$$

Using this approach with S_{in}/S_{out} = 0.96 (Lacombe and Tchernia, 1972), Harzallah et al. (1993) and Boukthir and Barnier (2000) obtained respectively 0.72 Sv and 0.77 Sv for the mean inflow. But equations [3] are very sensitive to small changes in the salinity ratio and S_{in}, S_{out} are not easy to determine, this causing large uncertainty. Our indirect approach avoids this problem and provides an intermediate value among those historically reported which is likely to be rather realistic since it combines reliable climatological and in situ datasets. Instead of using equation [3] for computing the inflow, we can use our values of G = 0.035 Sv and G_{in} = 0.82 Sv to determine a salinity ratio S_{in}/S_{out} = 0.956, slightly lower than the 0.96 adopted by Lacombe and Tchernia (1972), that can be used as a future reference when only a source of data (climatological or in situ) is available.

-----------------------------Approximate location of Table 6-----------------------------------

Unlike the water budget, the very reduced contribution of the Black Sea to the net heat budget can be neglected in all computations (Tolmazin, 1985). The Atlantic inflow through the Strait of Gibraltar is warmer than the Mediterranean outflow and it constitutes a positive heat advection Q_a given by:

$$Q_a = \rho C_p \{V_i T_i - V_o T_o - (ET_e - PT_p - RT_r)\} \quad [4]$$

where ρ is a reference water density, C_p the specific heat and T_i, T_o, T_e, T_p and T_r the mean temperature of inflow, outflow, evaporated water, precipitated water and river runoff. Assuming that T_e, T_p and T_r are not very different from T_o (which does not significantly alter the results, Garrett et al., 1993), Q_a can be expressed as:

$$Q_a = \rho C_p V_i (T_i - T_o) \quad [5]$$

We now compute this heat advection from in situ measurements and historical MEDATLAS CTD profiles (see section 2 for details). A mean temperature of T_o=13.25 ± 0.07 ºC has been obtained for the outflow from the CT probe. A spatially (within 35º 48.6’N – 35º 53.9’N / 05º 56.7’W – 06º 00.8’W, see Figure 1B) and depth-averaged temperature above the mean depth of the interface (186 m, Sanchez-Roman et al., 2009) of T_i=15.6 ± 1.1 ºC has been obtained for the inflow which implies a temperature difference of 2.4ºC. With these values and our mean estimation of 0.82 Sv for the inflow, a result of Q_a = 3.2 ± 1.5 Wm^{-2} is obtained for the heat advection. Although the value of 186 m for the mean depth of the interface is a well-documented choice (Sánchez-Román et al., 2009), the result for the heat advection is fairly robust and only small variations (less than 10%) have been observed for a wide range (150-200 m) of the mean interface.

This value is lower than historical reports that range from 8.5 Wm^{-2} (Béthoux, 1979) to 5 Wm^{-2} (Bunker et al., 1982) but is thought to be realistic since it comes from reliable datasets. The discrepancies with other results are probably due to a previous overestimation of the inflow (usually set to values above 1 Sv) since the temperature difference is rather similar. When combined with the long-term averaged surface net heat flux, this implies that the net heat content of the Mediterranean Sea would have increased in the last decades. This is compatible with the increment of deep water temperature reported by different authors (Rohling and Bryden, 1992; Bethoux and Gentili, 1999; López-Jurado et al., 2005; Font et al., 2007) and also with a positive thermosteric sea level trend (Criado-Aldeanueva et al., 2008). In any case, considering the uncertainty inherent to the estimation of surface heat fluxes, this result must be considered with caution.

4.- SUMMARY AND CONCLUDING REMARKS

We have used climatological datasets to analyse the seasonal and interannual variations of the components of heat and water budgets and compare the long term means with direct measurements in the Strait of Gibraltar.

The seasonal cycle of the net heat shows positive values (toward the ocean) between March and September with a maximum in June and negative values the rest of the year with a minimum in December. On a yearly basis, we obtain a nearly neutral budget of 0.7 Wm^{-2}. The net heat budget is positive (~12 Wm^{-2}) for the western Mediterranean and negative for the eastern Mediterranean (~ -6.4 Wm^{-2}) mainly due to the high latent heat losses of this basin (up to 100 Wm^{-2}). The E-P freshwater deficit has a seasonal cycle with a range of variation of about 600 mm·y^{-1}, a maximum in August-September and a minimum in May. The long-term mean of the basin-averaged deficit is 680±70 mm·y^{-1} but it is almost 70% higher in the eastern Mediterranean due to higher E and lower P in this basin. A positive trend (higher deficit) of 1.6±0.9 mm·y^{-2} is observed for the entire period in which the decrease in P seems to be the most important factor, although Mariotti (2010) also underlines the role of evaporation changes.

Reanalyses are useful for a comprehensive description of climate and related water/energy cycles, especially for describing climatological characteristics. However there is no constrain on the closure of the water and energy budgets at the level of the Mediterranen Sea, so there are uncertainties associated to results based on these products. Long-term variability is the less reliable aspect of reanalyses datasets as variability on these timescales may be affected by artifices (e.g. deriving from non-stationary data inputs). For this reason, the suggested long-period oscillation (40-year period) for P, E and E-P (and also for the net and latent heat) that could be related to long-term atmospheric forcing must de considered with caution. Despite of these caveats, the good agreement with other previous results in the literature makes them reliable for the estimation of the heat and water exchange through the Strait of Gibraltar.

Assuming a climatological river discharge and Black Sea contributions of 10.4·10^{3} m^{3}·s^{-1} (Struglia et al., 2004) and 8.8 · 10^{3} m^{3}·s^{-1} (Karnaska and Madirich, 2008), respectively, a mean net flow through the Strait of Gibraltar of 0.035 ± 0.005 Sv is obtained. From a 4 year-long time series of ADCP measurements over Espartel sill and results from a numerical model, a mean outflow of G_{out} = 0.78 ± 0.05 Sv is obtained (Sanchez-Roman et al., 2009), which implies a mean inflow ($G_{in} = G + G_{out}$) of 0.82 ±

0.05 Sv. Our result is an intermediate value among the few (due to technical and operational limitations) historically reported and is likely to be rather realistic since it comes from a combined climatological and in situ reliable dataset. Instead of using the conservation of salt for computing the inflow, which is subject to large uncertainty, we determine a salinity ratio S_{in}/S_{out} = 0.956 that can be used as a future reference when only one data source (climatological or in situ) is available.

With the above value for the inflow, a heat advection of Q_a = 3.2 ± 1.5 Wm^{-2} through the Strait of Gibraltar is obtained. This value, although lower than historical, is thought to be realistic, the discrepancies with other estimates being attributable to a previous overestimation of the inflow. This heat advection, along with the long-term averaged surface net heat flux, implies that the net heat content of the Mediterranean Sea would have increased in the last decades. This result, although subject to the uncertainty of the surface heat fluxes estimation, is compatible with the findings of Rohling and Bryden (1992), Bethoux and Gentili (1999), López-Jurado et al. (2005) and Font et al. (2007) who report an increment of deep water temperature and also with the positive thermosteric sea level trend observed by Criado-Aldeanueva et al. (2008).

ACKNOWLEDGEMENTS

This work has been carried out in the frame of the P07-RNM-02938 Junta de Andalucia Spanish-funded project. JSN acknowledges a postgraduate fellowship from Conserjería de Innovación Ciencia y Empresa, Junta de Andalucía, Spain. Partial support from CTM2006– 02326 (M. of Science and Technology) and P08-RNM-03738 (Junta de Andalucía) Spanish-funded projects are also acknowledged. NCEP and CMAP data have been provided by the NOAA/OAR/ESRL PSD, Boulder, Colorado, USA, from their website at http://www.esrl.noaa.gov/psd/. The SST data were obtained from the Physical Oceanography Distributed Active Archive Centre (PO.DAAC) at the NASA Jet Propulsion Laboratory, Pasadena, CA. http://podaac.jpl.nasa.gov. Both of them are acknowledged for free dissemination.

REFERENCES

Angelucci, M. G., N. Pinardi, and S. Castellari, 1998. Air–sea fluxes from operational analyses fields: Intercomparison between ECMWF and NCEP analyses over the Mediterranean area. Phys. Chem. Earth, 23, 569–574.

Astraldi M., F. Conversano, G. Civitarese, G. P. Gasparini, M. Ribera D'Alcalà, and A. Vetrano., 2002. Water mass properties and chemical signature in the central Mediterranean region. J. Marine Syst., 33-34: 155-177.

Baschek, B., Send, U., Lafuente, J.G., and Candela, J., 2001. Transport estimates in the Strait of Gibraltar with a tidal inverse model. Journal of Geophysical Research 106 (C12), 31033-31044.

Besiktepe, S. T., Sur, H.I., Ozsoy, E., Latif, M.A., Oguz, T., Unluata, U., 1994. The circulation and hydrography of the Marmara Sea.
Progress in Oceanography, 34 (4), pp. 285-334.

Bethoux, J.P, 1979. Budgets of the Mediterranean Sea: their dependence on the local climate and on the characteristics of Atlantic waters. Ocean. Acta 2, 157-163.

Bethoux, J.P. and Gentili B., 1999. Functioning of the Mediterranean Sea: Past and Present Changes realed to freshwater input and climatic changes. J. Mar. Syst. (20), 33-47.

Boukthir, M., and B. Barnier, 2000. Seasonal and inter-annual variations in the surface freshwater flux in the Mediterranean Sea from the ECMWF re-analysis project. J. Mar. Syst., (24), 343–354.

Bryden, H.L., Stommel, H.M., 1982. Origin of the Mediterranean outflow. Journal of Marine Research 40, 55–71.

Bryden, H. L., and T. H. Kinder, 1991a. Recent progress in strait dynamics. Rev. Geophys. (Suppl.), 617–631.

Bryden, H. L., and T. H. Kinder, 1991b. Steady two-layer exchange through the Strait of Gibraltar. Deep-Sea Res., 38S, 445–463.

Bryden, H. L., J. Candela, and T. H. Kinder, 1994. Exchange through the Strait of Gibraltar, Prog. Oceanogr., (33), 201–248.

Bunker, A.F., Charnock, H., Goldsmith, R.A., 1982. A note on the heat balance of the Mediterranean and Red Seas. J. Mar. Res. 40, 73-84, Suppl.

Candela, J., 2001. Mediterranean water and global circulation, in Ocean Circulation and Climate, edited by G. Siedler, J. Church, and J. Gould, pp. 419–429, Academic Press, San Diego, Ca.

Castellari, S., Pinardi, N., Leaman K., 1998. A model study of air-sea interactions in the Mediterranean Sea. J. Mar. Sys. 18, 89-114.

Cazenave, A., Bonnefond, P., Mercier, F., Dominh, K., Toumazou, V., 2002. Sea level variations in the Mediterranean Sea and Black Sea from satellite altimetry and tide gauges. Global and Planetary Change, (34), 59–86.

Criado-Aldeanueva F., Del Río Vera J., García-Lafuente J., 2008. Steric and mass induced sea level trends from 14 years altimetry data. Global and Planetary Change, (60), 563-575.

Fenoglio-Marc, L., 2002. Long-term sea level change in the Mediterranean Sea from multi-satellite altimetry and tide gauges. Physics and Chemistry of the Earth, (27), 1419–1431.

Fenoglio-Marc, L., Kusche J., Becker M., 2006. Mass variations in the Mediterranean Sea from GRACE and its validation by altimetry, steric and hydrologic fields. Geophys. Res. Lett., 33, L19606, doi:10.1029/2006GL026851.

Font, J., P. Puig, J. Salat, A. Palanques, M. Emelianov, 2007. Sequence of hydrographic changes in NW Mediterranean deep water due to the exceptional winter of 2005. Scientia Marina 71(2), 339-346.

García, D., Chao, B.F., Del Río, J., Vigo, I. 2006. On the steric and mass-induced contributions to the annual sea level variations in the Mediterranean Sea, J. Geophys. Res., 101, C09030, doi:10.1029/2006JC002956.

García Lafuente, J., J.M. Vargas, F. Plaza, T. Sarhan, J. Candela and B. Basheck 2000. Tide at the eastern section of the Strait of Gibraltar. J. Geophys. Res., 105, 14197-14213.

García Lafuente, J., J. Delgado, J.M. Vargas, M. Vargas, F. Plaza y T. Sarhan, 2002. Low-frequency variability of the exchanged flows through the Strait of Gibraltar during CANIGO. Deep Sea Res., 49, II, 4051-4067.

García-Lafuente, J., Sánchez-Román, A., Díaz del Río, G., Sannino, G., Sánchez-Garrido, J.C., 2007. Recent observations of seasonal variability of the Mediterranean outflow in the Strait of Gibraltar. Journal of Geophysical Research 112 C10, doi: 10.1029/2006JC003992.

García-Lafuente, J., Delgado, J., Sánchez-Román, A., Soto, J., Carracedo, L., Díaz del Río, G., 2009. Interannual variability of the Mediterranean outflow observed in

Espartel sill, western Strait of Gibraltar. Journal of Geophysical Research 114 C10, doi: 10.1029/2009JC005496.

Garrett, C., Outerbridge, R., Thompson, K., 1993. Interannual variability in Mediterranean heat and buoyancy fluxes. J. Climate 6, 900-910.

Garrett, C., 1996. The role of the strait of Gibraltar in the evolution of Mediterranean water, properties and circulation. Bull. Inst. Oceanogr. Mónaco 17, 1-19.

Gilman, C., Garrett, C., 1994. Heat flux parameterization for the Mediterranean Sea: the role of atmospheric aerosols and constraints from the water budget. J. Geophys. Res. 99 (C3), 5119-5134.

Jaeger, L., 1976. Monatskarten des Niederschlags fur die ganze Erde. Ber. Dtsch. Wetterdienstes, 18, 1–38.

Harzallah, A., D. L. Cadet, and M. Crepon, 1993. Possible forcing effects of net evaporation, atmospheric pressure and transients on water transports in the Mediterranean Sea. J. Geophys. Res., 98 (C7), 12 341–12 350.

Kalnay, E and co-authors (1996). The NCEP/NCAR 40-year reanalysis project. Bull. Amer. Meteor. Soc., 77:437-471.

Kanarska Y. and Maderich V., 2008. Modelling of seasonal Exchange flows through the Dardanelles Strait. Estuarine, Coastal and Shelf Science. (79), 449-458.

Lacombe, H., and P. Tchernia, 1972. Caracteres hydrologiques et circulation des eaux en Mediterranee. The Mediterranean Sea: A Natural Sedimentation Laboratory, D. J. Stanley, Ed., Dowden, Hutchinson and Ross, 25–36.

Lacombe H.; Richez C., 1982. The regime of the Strait of Gibraltar. In Hydrodynamics of Semi-Enclosed Seas. Ed. J.C.J. Nihoul. Amsterdam. 13-74.

Legates, D. R., and C. J. Wilmot, 1990. Mean seasonal and spatial variability in gauge-corrected, global precipitation. Int. J. Climatol., 10, 111–127.

List, R.J., 1951. Smithsonian Meteorological Tables, 6th rev. ed. Smithsonian Institute Press, 527 pp.

Liu, K.-K.; Atkinson, L.; Quiñones, R.; Talaue-McManus, L. (Eds.), 2009. Carbon and nutrients fluxes in continental margins, Global Change-The IGBP series. doi:10.1007/978-3-540-92735-2_7. Springer-Verlag. Berlin Heidelberg.

López-Jurado, J.L., González-Pola, C., Vélez-Belchí, P. 2005. Observation of an abrupt disruption of the long-term warming trend at the Balearic Sea, Western Mediterranean Sea, in summer 2005, Geophy. Res. Lett., 32, L24606, doi:10.1029/2005GL024430.

MacDonald, A.M., Candela, J., Bryden H.L, 1994. An estimate of the net heat transport through the Strait of Gibraltar, in Seasonal and Interannual variability of the Western Mediterranean Sea, Coastal Estuarine Stud., vol. 46, edited by P.E. LaViolette, pp. 12-32, AGU, Washington, D.C.

Margat, J., 1992. L'Eau dans le Bassin Mediterraneen: Situation et Perspective. Les Fascicules du Plan Bleu, No. 6, Economica, Paris, France, 196 pp.

Mariotti, A., Struglia, M.V., Zeng, N., Lau, K.-M., 2002. The hydrological cycle in the Mediterranean region and implications for the water budget of the Mediterranean Sea. Journal of Climate 15, 1674–1690.

Mariotti, A., Zeng, N., Yoon, J. H., Artale, V., Navarra, A., Alpert, P., Li, L.Z.X, 2008. Mediterranean water cycle changes: transition to drier 21st century conditions in observations and CMIP3 simulations. Environmental Research Letters 3 (4), 044001, doi: 10.1088/1748-9326/3/4/044001.

Mariotti A, 2010. Recent Changes in the Mediterranean Water Cycle: A Pathway toward Long-Term Regional Hydroclimatic Change? Journal of Climate 23 (6), 1513-1525.

Marullo, S., Santoleri, R., Malanotte-Rizzoli, P., Bergamasco, A., 1999. The sea surface temperature field in the eastern Mediterranean from advanced very high resolution radiometer (AVHRR) data. Part II: interannual variability. Journal of Marine Systems (20),83–112.

Matsoukas, C., Banks, A. C., Hatzianastassiou, N., Pavlakis, K. G., Hatzidimitriou, D., Drakakis, E., Stackhouse, P. W., Vardavas, I., 2005. Seasonal heat budget of the Mediterranean Sea. J. Geophys. Res., 110, C12008, doi:10.1029/2004JC002566.

May, P.W., 1986. A brief explanation of Mediterranean heat and momentum flux calculations. NORDA code 322, NSTL, MS 39529.

Millot, C., Candela, J., Fuda, J.-L., Tber, Y., 2006. Large warming and salinification of the Mediterranean outflow due to changes in its composition. Deep Sea Research 53/4, 656-666. doi:10.1016/j.dsr.2005.12.017.

Moron, V., 2003. L'évolution séculaire des températures de surface de la mer Méditerranée (1856–2000). Comptes Rendus Geoscience (335), 721–727 (in French with abridged English version).

Ovchinnikov, I.M., 1974. On the water balance of the Mediterranean Sea. Oceanology, 14, pp. 198-202.

Peixoto, J. P., M. De Almeida, R. D. Rosen, and D. A. Salstein, 1982. Atmospheric moisture transport and the water balance of the Mediterranean Sea. Water Resour. Res., 18, 83–90.

Rohling, E.J., Bryden, H.L., 1992. Man-induced salinity and temperature increases in western Mediterranean deep water. Journal of Geophysical Research 97 (C7), 11191–11198.

Ruiz S., Gomis D., Sotillo M. G., Josey S. A., 2008. Characterization of surface heat fluxes in the Mediterranean Sea from a 44-year high-resolution atmospheric data set. Global and Planetary change, (63), 256-274.

Ruti, P. M., Marullo, S., D'Ortenzio, F., Tremant, M., 2008 Comparison of analyzed and measured wind speeds in the perspective of oceanic simulations over the Mediterranean basin: Analyses, QuikSCAT and buoy data. Journal of Marine Systems 70, 33-48.

Sanchez-Román A., Sannino G., García-Lafuente J., Carillo A. and Criado-Aldeanueva F., 2009. Transport estimates at the western section of the Strait of Gibraltar: A combined experimental an numerical modeling study. Journal of Geophysical Research. (114), C06002, doi:10.1029/2008JC005023.

Schiano M.E., L. Santoleri, F. Bignami, R.M. Leonardo, Marullo and Bohm, 1993. Air-sea interactions measurements in the west Mediterranean Sea during the Thyrrhenian Eddy Multi-Platform Observations Experiments, J. Geophys. Res., 98(C2), 2461-2474.

Schroeder K., A. Ribotti, M. Borghini, R. Sorgente, A. Perilli, G.P. Gasparini, 2009. An extensive western Mediterranean deep water renewal between 2004 and 2006. Geophysical Research Letters 35(18), L18605.

Struglia M.V., Mariotti A. and Filograsso, 2004. River discharge into the Mediterranean Sea: Climatology and aspect of the Observed Variability. J. Climate. (17), 4740-51.

Tixeront, J., 1970. Le bilan hydrologique de la Mer Noire et de la mer Mediterranee. Cah. Oceanogr., 3, 227–237.

Tolmazin, D., 1985. Changing coastal oceanography in the Black Sea. I: Northwestern Shelf. Prog Oceanog.. 15.217-276.

Tsimplis, M.N. and Bryden, H., 2000. Estimation of the transports through the Strait of Gibraltar. Deep-Sea Research I, 47(12), 2219-2242.

Tziperman E. and Speer K., 1994. A study of mass transformation in the Mediterranean Sea: analysis of climatological data and simple three-box model. Dynamics of Atmospheres and Oceans. (21), 53-82.

UNESCO, 1996. Global River discharges database. Volume I: Africa, volume II: Asia, and volume III: Europe.

Unluata, U., Oguz, T., Latif, M.A., Ozsoy, E., 1990. On the physical oceanography of the Turkish Straits. The Physical Oceanography of Sea Straits. Nato/Asi Series, pp. 25-60. Pratt, L.J. (Ed.), Kluwer, Dordrecht.

Xie, P., and P. A. Arkin, 1996. Analysis of global monthly precipitation using gauge observations, satellite estimates, and numerical model predictions. J. Climate, 9, 840-858.

Xie, P., and P. A. Arkin, 1997. Global precipitation: A 17-year monthly analysis based on gauge observations, satellite estimates, and numerical model outputs. Bull. Amer. Meteor. Soc., (78), 2539–2558.

FIGURE CAPTIONS

Figure 1: A) Map of Mediterranean Sea. The main basins and subbasins are indicated. B) Zoom of the Strait of Gibraltar region. The rectangle indicates the area selected as representative for Espartel (ES).

Figure 2: A) Spatial distribution of climatological sea level air temperature (ºC) in the Mediterranean Sea for 1948-2009. B) Yearly time series of the basin-averaged air temperature (ºC, dotted line). The 5-year running mean is also plotted (solid line). C) Spatial distribution of air temperature linear trend ($ºC \cdot y^{-1}$) for 1948-2009. Panels D-F are the same but for SST during the period 1985-2007.

Figure 3: Seasonal climatology of the four components of the net heat budget in the Mediterranean for 1948-2009 (Wm^{-2}, positive toward ocean): sensible (panel A), latent (panel B), solar shortwave (panel C) and terrestrial longwave (panel D). In all panels: winter (top-left), spring (top-right), summer (bottom-left) and autumn (bottom-right).

Figure 4: Mediterranean-averaged climatological seasonal cycle for sensible heat (Q_h, grey dashed line), latent heat (Q_e, grey solid line), shortwave (Q_s, black dashed-dotted line) and longwave (Q_b, black dashed line) contributions for the period 1948-2009. Net heat seasonal cycle is also presented (Q_n, black solid line). Bars are the standard deviation.

Figure 5: A) Yearly Mediterranean-averaged time series of sensible heat (Q_h, grey dashed line), latent heat (Q_e, grey solid line), shortwave (Q_s, black dashed-dotted line), longwave (Q_b, black dashed line) and net heat flux (Q_n, black solid line) for the period 1948-2009. B) Latent (grey) and net (black) heat anomalies (yearly means, dotted; 5-year running means, solid). A multi-decadal oscillation is clearly suggested.

Figure 6: Seasonal climatology of P ($mm \cdot y^{-1}$, panel A), E ($mm \cdot y^{-1}$, panel B) and E-P ($mm \cdot y^{-1}$, positive means freshwater deficit, panel C) in the Mediterranean for 1948-2009. In all panels: winter (top-left), spring (top-right), summer (bottom-left) and autumn (bottom-right).

Figure 7: Mediterranean-averaged climatological seasonal cycle of E (black solid line), P (dotted lines, black for NCEP and grey for CMAP) and E-P (dashed-dotted lines, black for NCEP and grey for NCEP (E)/CMAP (P)) for the periods 1948-2009 (NCEP) and 1979-2009 (CMAP). Bars are the standard deviation. Labels indicating each cycle are also shown for clarity.

Figure 8: Spatial distribution of annual amplitude ($mm \cdot y^{-1}$) and phase (degrees) of the main surface freshwater fluxes contributions: A) P annual amplitude (NCEP); B) P annual amplitude (CMAP); C) E annual amplitude; D) E-P annual amplitude (NCEP); E) E-P annual amplitude (NCEP (E)/CMAP (P)) and F) E-P annual phase (NCEP).

Figure 9: A) Yearly Mediterranean-averaged time series of E (black solid line), P (dotted lines, black for NCEP and grey for CMAP) and E-P (dashed-dotted lines, black for NCEP and grey for NCEP (E)/CMAP (P)). B) Anomalies (yearly means, dotted; 5-year running means, solid) are shown in this panel (E top, P middle, E-P bottom) to highlight the interannual variability. The multi-decadal oscillation is clearly suggested.

TABLES

	Mean			Winter			Spring			Summer			Autumn		
	Med	**Wm**	**Em**	**Med**	**Wm**	**Em**	**Med**	**Wm**	**Em**	**Med**	**Wm**	**Em**	**Med**	**Wm**	**Em**
Q_h	-15.1	-13.3	-16.2	-27.6	-22.3	-30.8	-1.5	-2.0	-1.2	-3.8	-3.7	-3.8	-27.6	-25.0	-29.1
Q_e	-93.5	-78.4	-103.4	-99.4	-82.3	-110.5	-57.9	-48.5	-64.0	-93.9	-75.9	-105.6	-123.1	-107.2	-133.5
Q_s	186.3	176.7	192.3	133.9	125.3	139.2	254.6	246.2	259.8	245.0	233.7	252.0	112.3	101.9	118.8
Q_b	-76.9	-73.1	-79.3	-76.9	-74.1	-78.6	-75.9	-71.5	-78.5	-78.8	-73.9	-81.8	-76.2	-72.9	-78.2
Q_n	0.73	11.7	-6.4	-70.0	-53.5	-80.7	120.0	120.0	120.0	69.6	80.1	61.1	-110.0	-100.0	-120.0

Table 1: Mediterranean (Med) long term mean heat fluxes contributions (Wm^{-2}). Values for the western (Wm) and eastern (Em) basins are shown for each season.

Authors	Q_h	Q_e	Q_s	Q_b	Q_n	**Period**
Bethoux (1979)	-13	-120	195	-68	-6	Not specified
Bunker et al. (1982) (1)	-13	-101	202	-68	20	1941-1972
Bunker et al. (1982) (2)	-11	-130	202	-68	-7	1941-1972
May (1986)	-11	-112	193	-68	2	1945-1984
Garrett et al. (1993)	-7	-99	202	-67	29	1946-1988
Gilman and Garrett (1994)	-7	-99	183	-77	0	1946-1988
Castellari et al. (1998)	-13	-122	202	-78	-11	1980-1988
Matsoukas et al. (2005)	-11	-90	186	-63	22	1984-2000
Ruiz et al. (2008)	-8	-88	168	-73	-1	1958-2001
This work	-15	-93	186	-77	1	1948-2009

Table 2: Mediterranean long term mean heat budget (Wm^{-2}) estimated by different authors. The periods to which the estimates refer are also indicated.

				Winter			Spring			Summer			Autumn		
	Med	Wm	Em	Med	Wm	Em	Med	Wm	Em	Med	Wm	Em	Med	Wm	Em
E	1186	1011	1296	1256	1061	1378	745	625	820	1193	979	1330	1553	1382	1559
P(NCEP)	506	527	491	675	630	702	249	281	232	245	299	209	853	897	818
P(CMAP)	469	517	442	614	551	649	305	415	244	205	312	145	754	790	734
E-P (NCEP)	680	484	806	581	430	676	495	345	589	947	680	1121	700	485	841
E-P (NCEP/CMAP)	678	497	777	597	479	663	418	212	532	922	681	1055	780	623	867

Table 3: Mediterranean (Med) long term mean freshwater contributions ($mm \cdot y^{-1}$). Values for the western (Wm) and eastern (Em) basins are shown for each season. For E-P computation from CMAP P dataset, only the period 1979-2009 of NCEP E time series has been used.

Authors	E	P	E-P	Method
Tixeront (1970)	1200	350	850	Observations and assumptions
Jaeger (1976)	1210	550	660	Derived from observations
Gilman and Garrett (1994)	1121-1430	550(1)-700(2)	421-880	Derived from observations
Angelucci et al. (1998)	1100	450	650	Analyses, ECMWF/NCEP
Castellari et al. (1998)	1320-1570	550(1)-700(2)	620-1020	Derived from observations
Bethoux and Gentili (1999)	1360-1540	310	1050-1230	Derived from observations
Boukthir and Barnier (2000)	920	326	594	Reanalyses, ECMWF 1979-1993
Mariotti et al. (2002)	1171	504	667	Reanalyses, NCEP 1948-1998
Mariotti et al. (2002)	1113	433	680	Reanalyses, NCEP 1979-1993
Mariotti et al. (2002)	934	331	603	Reanalyses, ECMWF 1979-1993
Mariotti et al. (2002)	1176	477	699	UWM/COADS, CMAP 1979-1993
This work	1186	506/469	680/678	Reanalyses, NCEP 1948-2009/CMAP 1979-2009

Table 4: Climatological contributions to the Mediterranean water budget ($mm \cdot y^{-1}$) estimated by different authors. (1): Adopted from Jaeger (1976); (2): Adopted from Legates and Wilmott (1990).

Authors	G	Method
Lacombe and Tchernia (1972)	0.054	Current observations at Gibraltar
Bethoux (1979)	0.079	Ocean potential energy budget
Bryden and Kinder (1991a)	0.040-0.048	Current observations and salt budget
Bryden and Kinder (1991b)	0.040-0.050	Ocean model simulation
Bryden et al. (1994)	0.041	Current observation and salt budget
Garrett (1996)	0.041	Modelling at Gibraltar
Boukthir and Barnier (2000)	0.031	Water budget from ERA-15
Candela (2001)	0.04	Current observations at Gibraltar
Mariotti et al. (2002)	0.039	Water budget from several datasets
This work	0.035	Water budget from several datasets

Table 5: Annual mean of net water transport through the Strait of Gibraltar (Sv, 1Sv = 10^6 $m^3 \cdot s^{-1}$) as estimated by different authors.

Authors	G_{in}	Period of observations
Lacombe and Richez (1982)	1.2	09/60 – 06/61
Bryden et al (1994)	0.72	1985 – 1986
Tsimplis and Bryden (2000)	0.78	01/97– 04/97
García Lafuente et al (2000)	0.92	10/95 – 04/96
Baschek et al (2001)	0.81	Various intervals between 10/94 and 04/97
Candela (2001)	1.01	1995-1996
García Lafuente et al (2002)	0.96	Various intervals between 10/95 and 05/98
This work	0.82	09/04 – 12/08

Table 6: Mean inflow through the Strait of Gibraltar (Sv, 1Sv = 10^6 $m^3 \cdot s^{-1}$) as estimated by different authors.

FIGURES

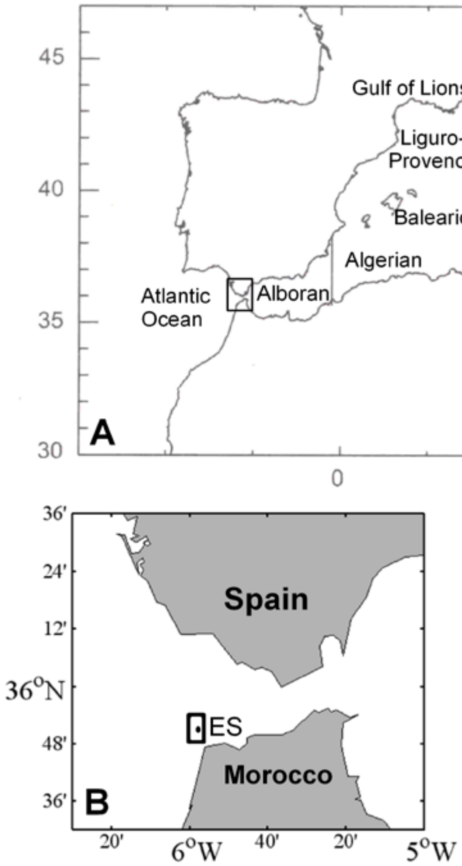

Figure 1: A) Map of Mediterranean Sea. The main basins and subbasins are indicated. B) Zoom of the Strait of Gibraltar region. The rectangle indicates the area selected as representative for Espartel (ES).

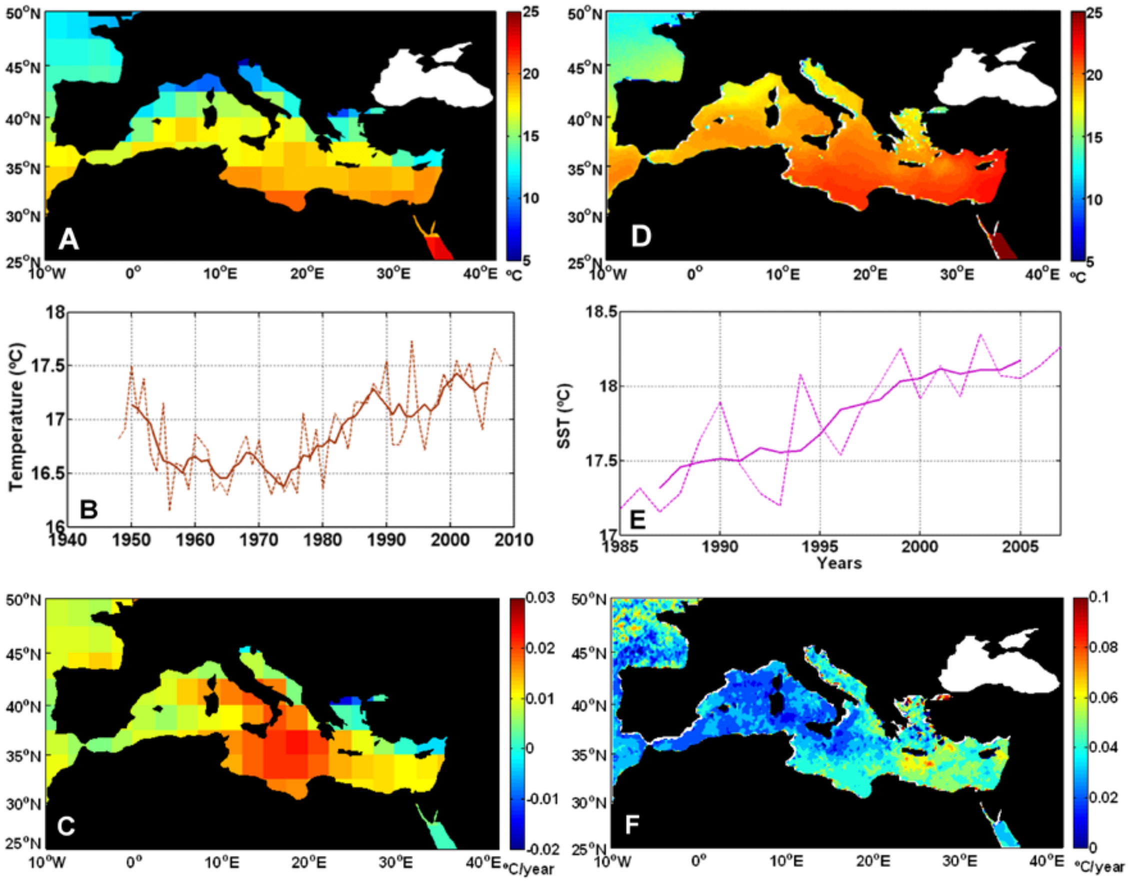

Figure 2: A) Spatial distribution of climatological sea level air temperature (ºC) in the Mediterranean Sea for 1948-2009. B) Yearly time series of the basin-averaged air temperature (ºC, dotted line). The 5-year running mean is also plotted (solid line). C) Spatial distribution of air temperature linear trend (ºC·y^{-1}) for 1948-2009. Panels D-F are the same but for SST during the period 1985-2007.

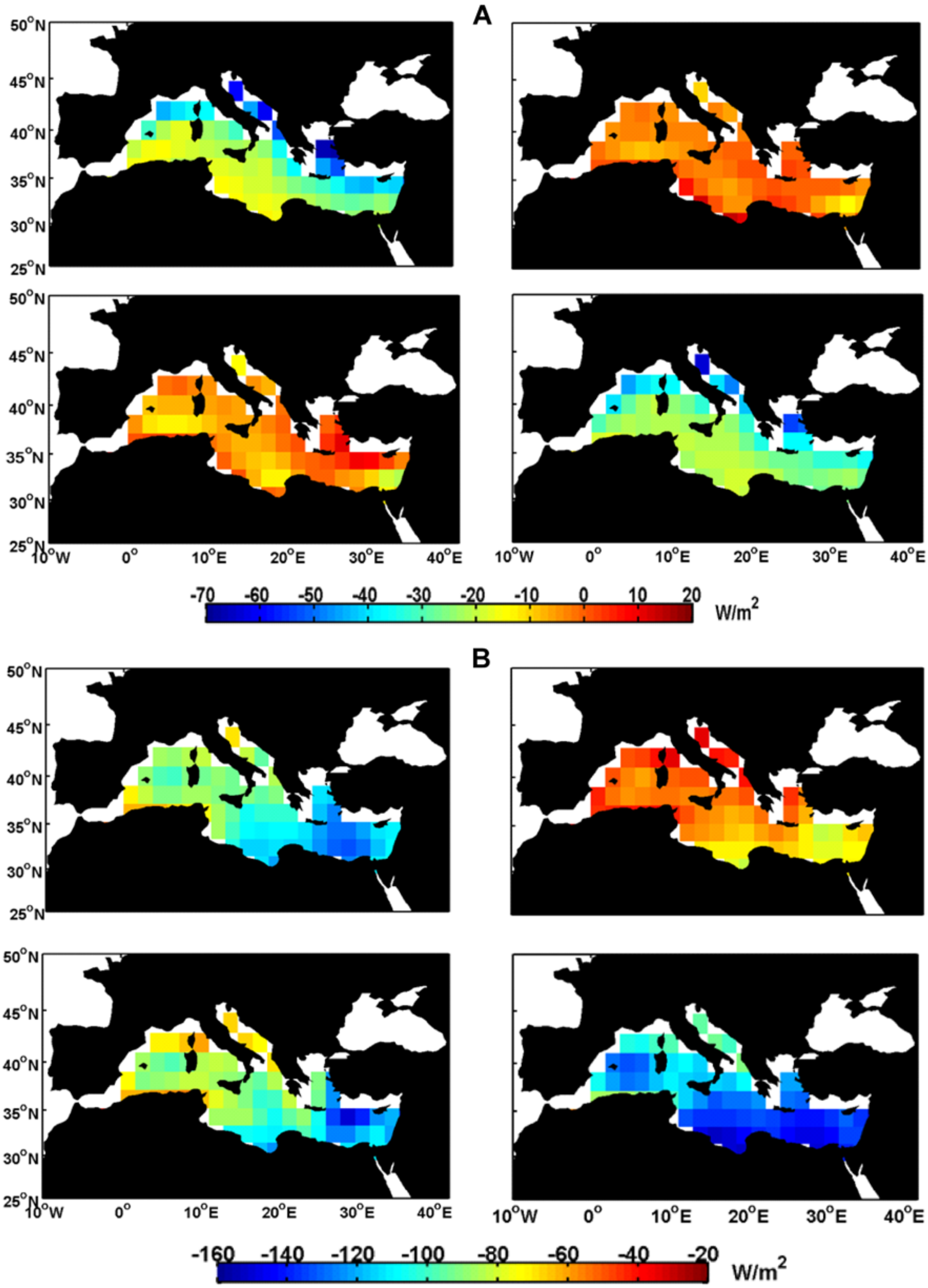

Figure 3: Seasonal climatology of the four components of the net heat budget in the Mediterranean for 1948-2009 (Wm^{-2}, positive toward ocean): sensible (panel A), latent (panel B), solar shortwave (panel C) and terrestrial longwave (panel D). In all panels: winter (top-left), spring (top-right), summer (bottom-left) and autumn (bottom-right).

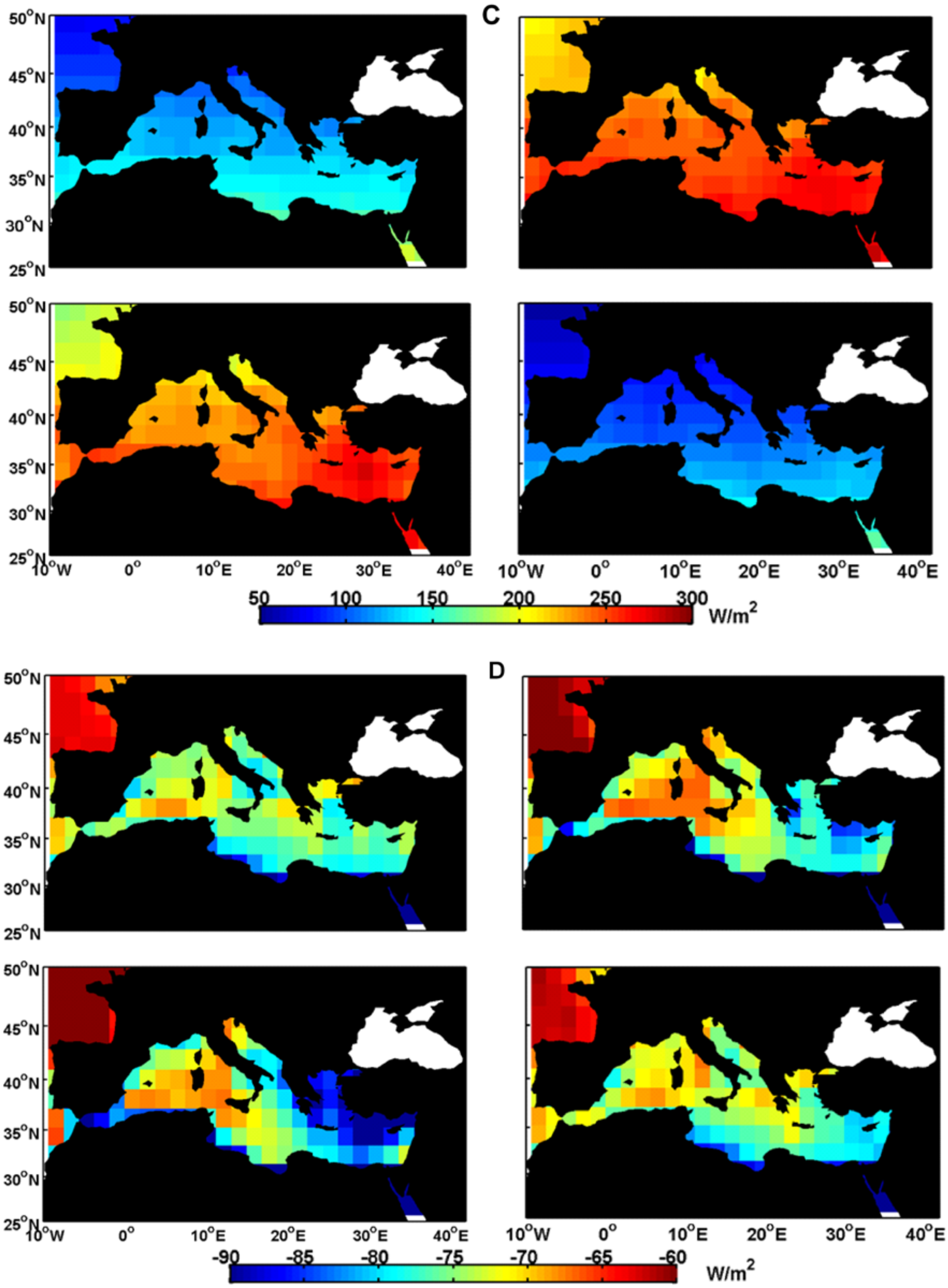

Figure 3 (cont)

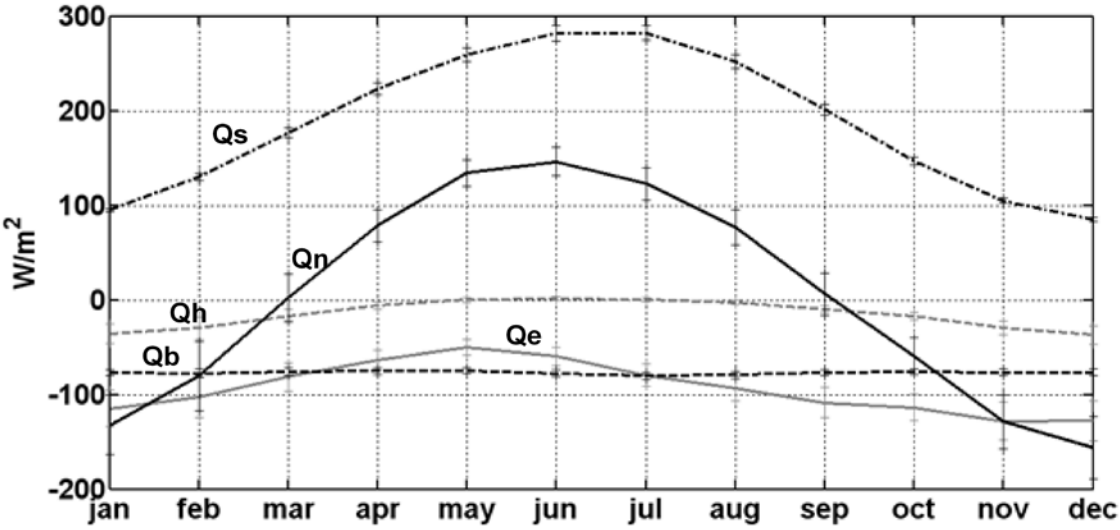

Figure 4: Mediterranean-averaged climatological seasonal cycle for sensible heat (Q_h, grey dashed line), latent heat (Q_e, grey solid line), shortwave (Q_s, black dashed-dotted line) and longwave (Q_b, black dashed line) contributions for the period 1948-2009. Net heat seasonal cycle is also presented (Q_n, black solid line). Bars are the standard deviation.

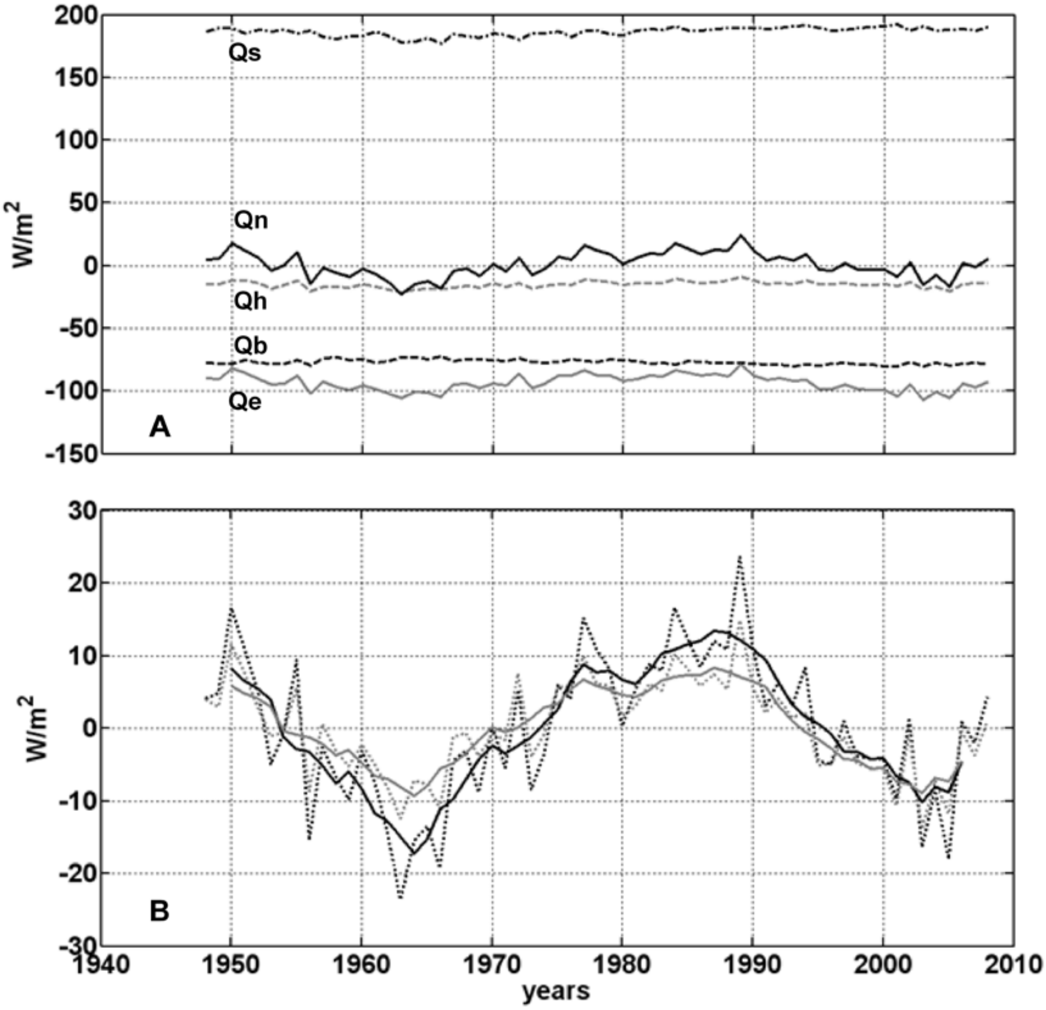

Figure 5: A) Yearly Mediterranean-averaged time series of sensible heat (Q_h, grey dashed line), latent heat (Q_e, grey solid line), shortwave (Q_s, black dashed-dotted line), longwave (Q_b, black dashed line) and net heat flux (Q_n, black solid line) for the period 1948-2009. B) Latent (grey) and net (black) heat anomalies (yearly means, dotted; 5-year running means, solid). A multi-decadal oscillation is clearly suggested.

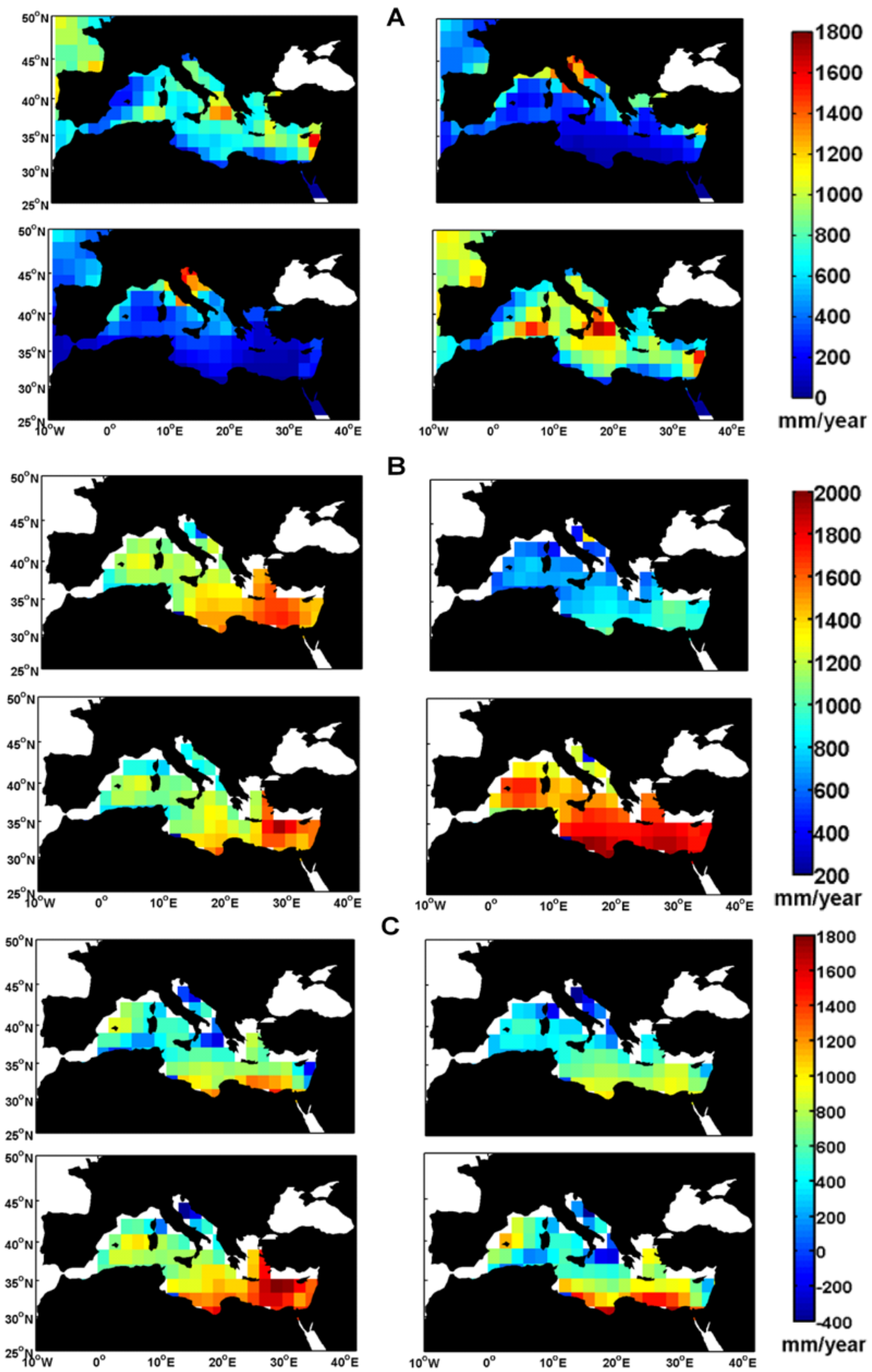

Figure 6: Seasonal climatology of P ($mm\cdot y^{-1}$, panel A), E ($mm\cdot y^{-1}$, panel B) and E-P ($mm\cdot y^{-1}$, positive means freshwater deficit, panel C) in the Mediterranean for 1948-2009. In all panels: winter (top-left), spring (top-right), summer (bottom-left) and autumn (bottom-right).

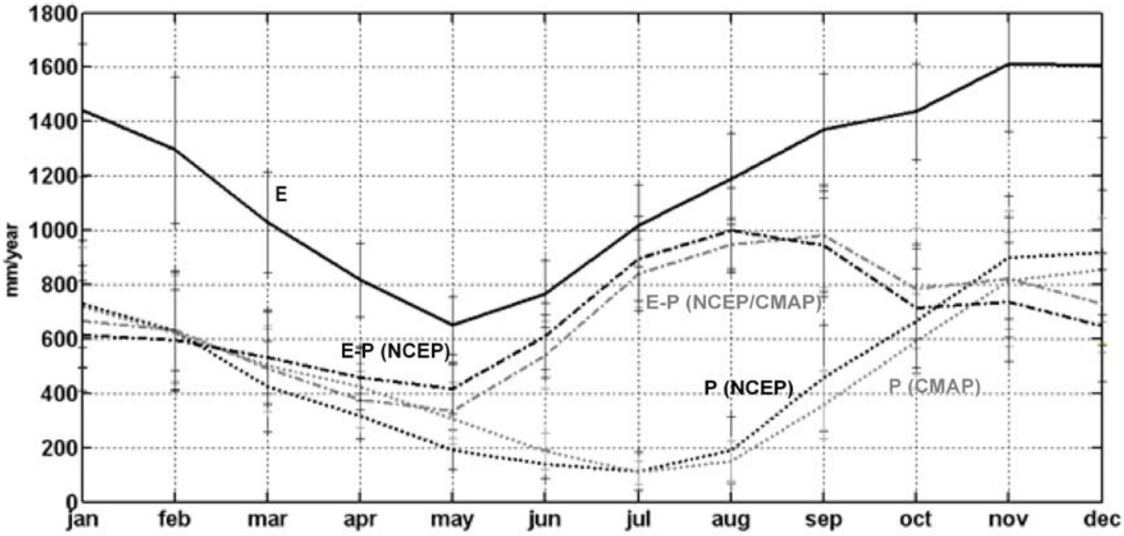

Figure 7: Mediterranean-averaged climatological seasonal cycle of E (black solid line), P (dotted lines, black for NCEP and grey for CMAP) and E-P (dashed-dotted lines, black for NCEP and grey for NCEP (E)/CMAP (P)) for the periods 1948-2009 (NCEP) and 1979-2009 (CMAP). Bars are the standard deviation. Labels indicating each cycle are also shown for clarity.

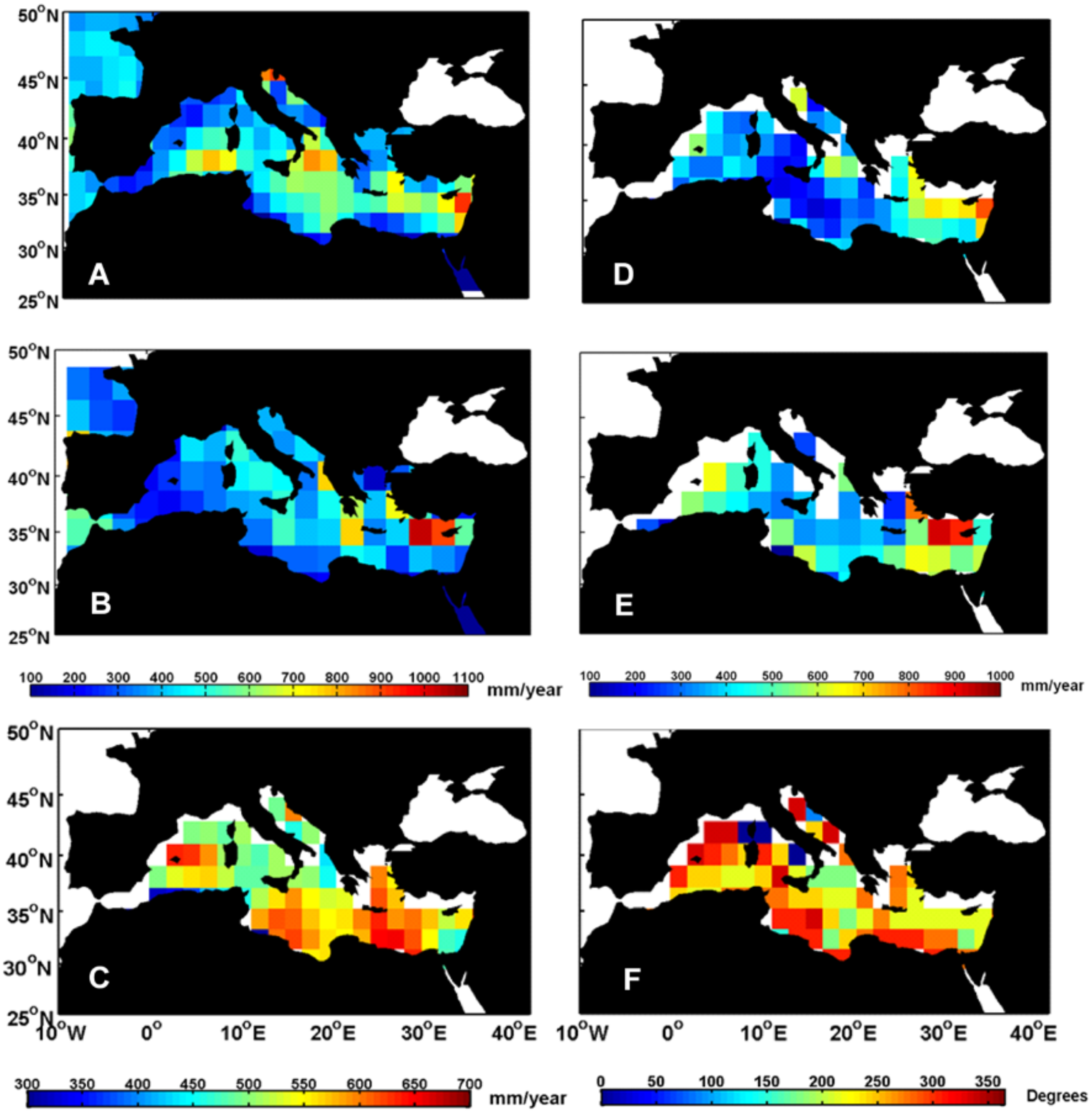

Figure 8: Spatial distribution of annual amplitude ($mm \cdot y^{-1}$) and phase (degrees) of the main surface freshwater fluxes contributions: A) P annual amplitude (NCEP); B) P annual amplitude (CMAP); C) E annual amplitude; D) E-P annual amplitude (NCEP); E) E-P annual amplitude (NCEP (E)/CMAP (P)) and F) E-P annual phase (NCEP).

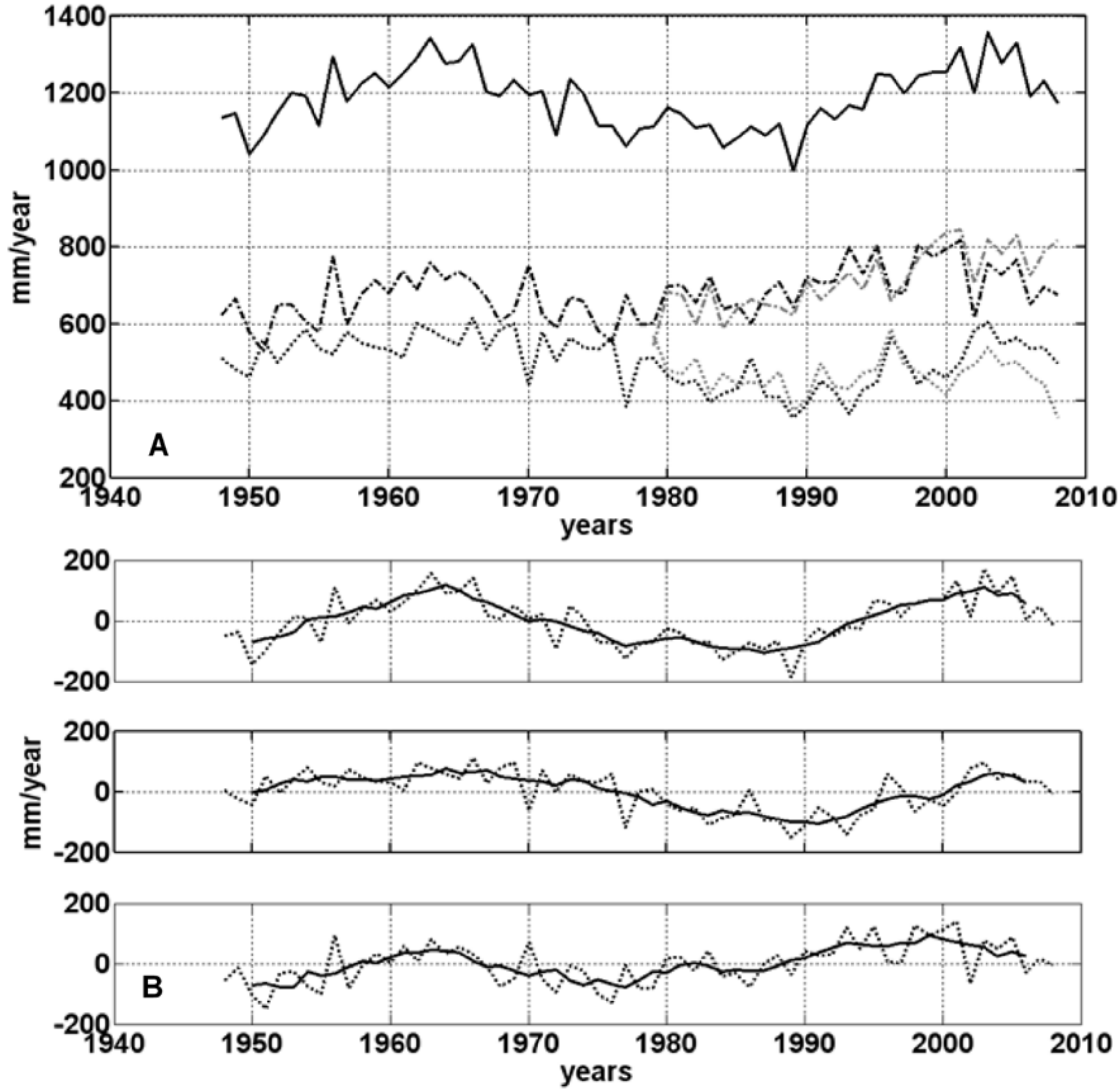

Figure 9: A) Yearly Mediterranean-averaged time series of E (black solid line), P (dotted lines, black for NCEP and grey for CMAP) and E-P (dashed-dotted lines, black for NCEP and grey for NCEP (E)/CMAP (P)). B) Anomalies (yearly means, dotted; 5-year running means, solid) are shown in this panel (E top, P middle, E-P bottom) to highlight the interannual variability. The multi-decadal oscillation is clearly suggested.